



# 3D numerical modelling of underground excavations in a faulted rock mass using the Boundary Elements Method (BEM)

Mamoudou Sylla, Marwan Al Heib, Jack-Pierre Piguet

## ► To cite this version:

Mamoudou Sylla, Marwan Al Heib, Jack-Pierre Piguet. 3D numerical modelling of underground excavations in a faulted rock mass using the Boundary Elements Method (BEM). 53. Canadian Geotechnical Conference, Oct 2000, Montréal, Canada. ineris-00972204

**HAL Id: ineris-00972204**

**<https://hal-ineris.archives-ouvertes.fr/ineris-00972204>**

Submitted on 3 Apr 2014

**HAL** is a multi-disciplinary open access archive for the deposit and dissemination of scientific research documents, whether they are published or not. The documents may come from teaching and research institutions in France or abroad, or from public or private research centers.

L'archive ouverte pluridisciplinaire **HAL**, est destinée au dépôt et à la diffusion de documents scientifiques de niveau recherche, publiés ou non, émanant des établissements d'enseignement et de recherche français ou étrangers, des laboratoires publics ou privés.

# 3D numerical modelling of underground excavations in a faulted rock mass using the Boundary Elements Method (BEM)

## Applications to the Provence colliery

M. Sylla\*, M. Al Heib\*\*, J.P. Piguet\*

\*LAEGO : Laboratoire Environnement, Géomécanique et Ouvrages. Ecole des Mines de Nancy - France

\*\*INERIS : Institut National de l'Environnement Industriel et des Risques. Ecole des Mines de Nancy - France

### Abstract :

This paper presents a 3D-numerical modelling technique for underground excavations in a faulted rock mass. The displacement discontinuity method is used to solve the differential equation of the problem. A presentation of this method is given in the first part of the paper. The second aspect of this paper is concerned with the verification of the new code by comparison with the results obtained from commercial numerical codes UDEC (distincts elements) and CESAR (finites elements). Case study involving a coal mining panel excavation in a faulted rock mass is presented to demonstrate the application of the code to practical mine problems.

### Résumé :

Ce papier présente le développement d'un code de modélisation numérique permettant de calculer les contraintes induites par une exploitation souterraine en présence de failles. La méthode des discontinuités de déplacement est utilisée pour résoudre l'équation différentielle du problème. Une présentation de cette méthode et son utilisation pour modéliser des veines et des failles sont présentées dans la première partie de cet article. Ensuite, une vérification de ce code, par comparaison aux codes de calculs UDEC (éléments distincts) et CEASR (élément finis), est proposée. Enfin, une étude de cas portant sur l'exploitation d'un nouveau panneau en présence de failles dans la mine de Provence (Sud de la France) est menée pour confronter les résultats obtenus à un cas réel.

### Introduction :

The presence of faults in the rock mass surrounding underground mines can cause failure and even major rockbursts due to sliding on fault planes. Therefore, for safety and economic reason, it is necessary to be able to predict the behaviour of a mining zone, particularly, when it is situated in a faulted area. To achieve this goal, the authors have recently developed a 3D numerical modelling code (FAULT3D) using the Boundary Element Method (BEM).

Model input parameters include rock mass parameters (Young modulus, Poisson's ratio, unit weight, initial or in situ stresses), fault characteristics (tensile strength, cohesion, friction angle, normal and shear stiffness), mine geometry (panels and faults). A method to treat underground voids (gob or backfill) was developed. A 2 or 3 dimensional geometry view is available.

The BEM requires to calculate and to solve a system of equations resulting from the influence of all the boundary elements. That is quite a big advantage compared to an equivalent differential method but it rapidly becomes inefficient when we deal with a large number of openings and/or faults. To overcome this problem, we propose an iterative method which allows us to significantly increase the number of boundary elements and consequently the number of panels and faults by making the calculation separately for each fault and for each opening. During the iteration procedure, stress corrections are done in fault planes, with respect to two criteria, in order to account for permanent traction or shear failure (Mohr-Coulomb criteria for shear failure).

The code FAULT3D is presented herein, together with the scheme of calculation. A model verification was carried out by comparison with a two dimensional model constructed with UDEC 2.0 and CESAR - LCPC 3.1. An application to the Provence coal mine location, is also presented to demonstrate the practical application of the new code.

## 1 Displacement discontinuities method (DDM)

The displacement discontinuity method is a variant of the boundary elements method for solving problems in solid mechanics in general [2]. It is particularly appropriate for problems involving faults or joints, mining in tabular orebodies (which extend at most a few meters in one direction and hundreds to thousands in the two others). We only need to suppose, for both faults and panels in tabular orebodies, that the boundary consists of two parts very close proximity to each other. The displacement discontinuity represents the relative displacement between the two sides of the boundary and has a physical meaning such as the closure of a mined excavation or the slip on a fault plan.

Let  $S$  represent a discontinuity surface within an elastic, homogenous, isotropic and infinite solid (Figure 1).

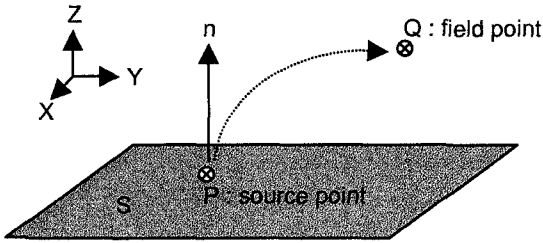


Figure 1 : Definition of the displacement discontinuity

From the general theory [4], it follows that the induced stresses at any field point  $Q$  are given by the integral :

$$\sigma_{ij}^{ind}(Q) = \frac{E}{8\pi(1-\nu^2)} \int_S R_{ijk}(P, Q) \Delta U_k(P) ds \quad [1]$$

$i, j, k = X, Y, Z$

$\sigma^{ind}(Q)$  : induced stresses tensor at the field point  $Q$ .

$\Delta U_k = U_k^+ - U_k^-$  :  $k^{th}$  displacement discontinuity component at the integration point  $P$ .

$U^+$  ( $U^-$ ) is a limit value of displacements when approaching  $S$  from the side for which the normal to the surface at the point  $P$  is an outward (inward) normal.

$R$  : influence coefficient of the integration point  $P$  on the field point  $Q$ .

$E$  : Young's modulus.

$\nu$  : Poisson's ratio.

If  $Q$  is tending to a point  $Q_0$  of the surface  $S$ , we obtain in the limit of the surface :

$$T_i^{ind}(Q_0) = \frac{E}{8\pi(1-\nu^2)} \int_S R_{ijk}(Q_0, P) n_j(Q_0) \Delta U_k(P) ds \quad [2]$$

where  $T^{ind}(Q_0) = \begin{bmatrix} \sigma_n \\ \tau_1 \\ \tau_2 \end{bmatrix} = \sigma_{ij}^{ind}(Q_0) \cdot n_j(Q_0)$ ,  $\sigma_n$  is the traction the normal to the surface.

$\tau_1$  and  $\tau_2$  are the shear traction boundary at the point  $Q_0$ ,  $n_j(Q_0)$  is the  $j^{th}$  component of the normal to the surface at the point  $Q_0$ .

Let us write  $S$  as a sum of  $N$  elements  $\left( S = \bigcup_{p=1}^N S_p \right)$ .

Each of them is called a displacement discontinuity element. The induced traction at the  $Q^{th}$  element ( $Q = 1, \dots, N$ ) is obtained from [2] by :

$$T_i^{ind}(Q) = \frac{E}{8\pi(1-\nu^2)} \sum_{p=1}^N \left[ \int_{S_p} R_{ijk}(Q, P) \cdot n_j(Q) ds \right] \Delta U_k^p \quad [3]$$

$i, j, k = X, Y, Z$

$\Delta U^P$  : is the constant displacement vector at the  $P^{th}$  element.

If we know a method to evaluate the integrals over the elements, and if the displacement discontinuity vector at each element (3 components) is known we can find using relation [3] the traction boundary induced vector at any point in the surface.

In the next section, we explain how to use this method to analyse mining rock mechanics problems involving major discontinuities or faults

## 2 Use of DDM in mining rock mechanics problems

The key concept underlying the DDM is considering the tabular deposit or the fault plane as a discontinuity in a homogeneous, isotropic, linear elastic rock mass. DDM, unlike other numerical methods (finite elements for example) only requires the subdivision of the problem boundary (tabular deposit or fault plane) into elements instead of meshing the whole rock mass. Thus, it requires much less computational effort than any other equivalent differential method.

The boundary elements are considered in two different ways depending if they belong to a mined area or a fault plan. In the first case, we assume that one face corresponds to the roof and the second to the floor of the excavation. In the second case, we suppose that the opposite face of a discontinuity are connected with springs whose normal and shear stiffnesses are known.

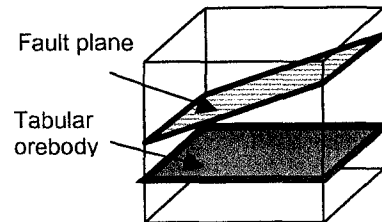


Figure 2 : Typical mining problem solved by the DDM

## 2.1 Mined area

We can say that the total stress in an element, let us say  $q$ , is obtained as the sum of the initial stresses and the induced stresses by all the elements in the mined area. For these elements, the total stresses are zero. We have,

$$T^{Tot} = T^0 + T^{ind} = 0$$

$$-T_i^0(Q) = \frac{E}{8\pi(1-\nu^2)} \sum_{P=1}^N \left[ \int_{S_P} n_j(Q) R_{ijk}(Q, P) ds \right] \Delta U_k^P \quad [4]$$

$$Q = 1, \dots, N, i, j, k = X, Y, Z$$

This leads us to a system of  $3 \times N$  equations with  $3 \times N$  unknowns (three components of the displacement discontinuity vector for each element). If we suppose that the initial traction vector (3 components) in each element is known and have a method to evaluate the integrals over the elements, we can use an appropriate method to solve the system [5] to find the displacement discontinuity at each element. Using this solution, we can find via the integral [1] the complete induced stress tensor at any field point around the mine opening.

## 2.2 Fault plane

In this case, it was assumed that the fault does not slip until the excavation is made in its vicinity. For modelling purpose, a fault can be considered to be filled by a compressible material. Thus, the opposite faces of each fault elemental displacement discontinuity can be modelled to be connected by a spring chosen to be representative of the properties of the filling material (Goodman, 1976). The value of the displacement discontinuity components at each element, therefore, will be related to the normal and the shear stresses acting on it.

The normal and the shear induced boundary tractions can be related by the stiffness matrix to displacement discontinuity by (K. Fotoohi, 1993) [3]:

$$T^{ind} = \begin{bmatrix} \sigma_n^{ind} \\ \tau_1^{ind} \\ \tau_2^{ind} \end{bmatrix} = \begin{bmatrix} K_n & 0 & 0 \\ 0 & K_s & 0 \\ 0 & 0 & K_s \end{bmatrix} \begin{bmatrix} \Delta U_x \\ \Delta U_y \\ \Delta U_z \end{bmatrix} \quad [5]$$

From (3) we can write,

$$\begin{bmatrix} K_n & 0 & 0 \\ 0 & K_s & 0 \\ 0 & 0 & K_s \end{bmatrix} \begin{bmatrix} \Delta U_x \\ \Delta U_y \\ \Delta U_z \end{bmatrix} = \frac{E}{8\pi(1-\nu^2)} \sum_{P=1}^N \left[ \int_{S_P} R_{ijk}(Q, P) n_j(Q) ds \right] \Delta U_k^P \quad [6]$$

$$0 = \frac{E}{8\pi(1-\nu^2)} \sum_{P=1}^N \left[ \int_{S_P} R_{ijk}(Q, P) n_j(Q) ds \right] + \frac{8\pi(1-\nu^2)}{E} \delta_{PQ} \delta_{ij} \Delta U_k^P$$

Where,  $\delta_{ij} = 1$  if  $i=j$  otherwise,  $S_k = K_n$  if  $k=X$  and  $S_k = K_s$  if  $k=Y$  or  $Z$ .  
 $Q = 1, \dots, N$ .

It simply corresponds to add  $K_n$  and  $K_s$  to the diagonal terms of the fault's influence matrix. The left side of the system is zero in respect with the assumption that there is no fault plan displacement before the excavation.

Consideration of the non-linear behaviour of the faults should lead us to more realistic results. For this purpose, two criteria have been chosen. These are presented below.

### 2.2.1 Tensile strength failure : $\sigma_n < R_t$

The normal stress  $\sigma_n$  on DD fault element can not exceed its tensile strength ( $R_t$ ). When this condition is reached in DD element, the fault is considered open and acts exactly like an element on the boundary of an opening (Total stresses are zero).

### 2.2.2 Shear strength failure : $\tau < C + \sigma_n \tan(\phi)$

The Mohr-Coulomb condition is chosen to model the shear behaviour of the fault. The meaning of this constraint is that the total shear stress cannot exceed a certain amount given by the relation  $C + \sigma_n \tan(\phi)$ , where  $C$  is the cohesion of the fault,  $\phi$  its friction angle and  $\sigma_n$  the normal stress acting on the fault surface. If an element fails according to this criterion, the fault is considered in permanent slip and the excess shear stress is taken as the new boundary condition in the relation [7] instead of zero.

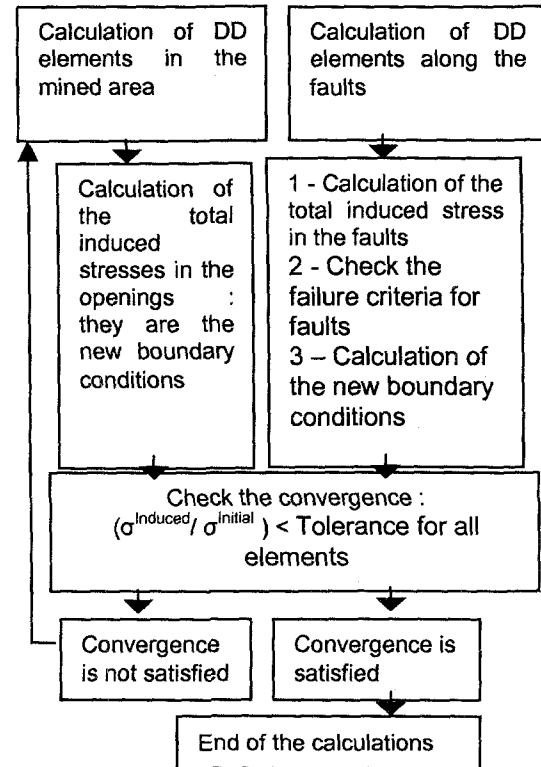


Figure 3 : flowchart of calculation in FAULT3D

### 3 Verification of the code

In this section a verification of FAULT3D code is presented by comparison with the distinct element code UDEC 2.0 and the finite element code CESAR-LCPC 3.1. Two models involving the mining of a single panel, are presented here (figure 4). The width of the panel is fixed to 200 m and is 1000 m long, thus to justify plane stress analysis. The seam depth is 1000 m. In the first case, we consider two faults parallel to the panel, along its length, and in the second one, only one of the two faults is parallel to the panel. The results of a two dimensional modelling depend, in the latter, on where the cross section is chosen.

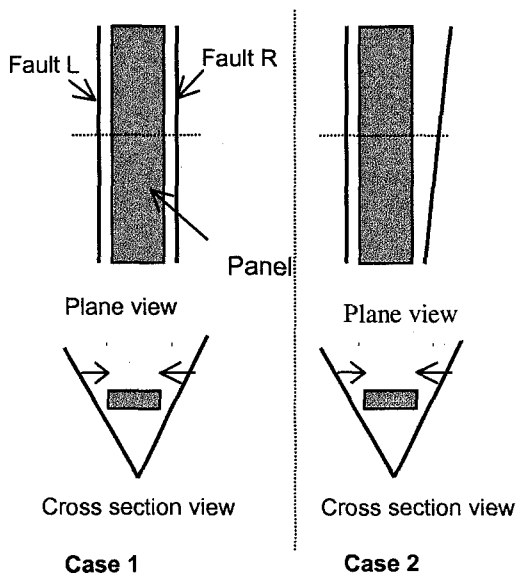


Figure 4 : Definition of model verification code

#### Rock mass properties :

The elastic rock parameters are : Young's modulus 10,000 MPa, Poisson's ratio 0.1 and unit weight 0.025 MN/m<sup>3</sup>.

#### Faults parameters :

The above data present the geomechanic parameters of the two faults.

	C (MPa)	$\Phi$ (°)	$R_t$ (MPa)	$K_n$ (MPa/m)	$K_s$ (MPa/m)
Fault L	0	30	0	10 000	1000
Fault R	0	10	0	10 000	1000

#### In situ stresses

The initial stresses correspond to the overall virgin stress field. It is assumed that they are not modified by the tectonic activity nor by faulting. At this depth (1000 m) and with a unit weight equal to 0.025 MN/m<sup>3</sup>, the in situ stresses are :  $\sigma_v = \sigma_{E-W} = \sigma_{N-S} = 25$  MPa

### 3.2 Analysis of the results

Figure 5 shows that only the bottom part of the right fault is on shear failure. This part lies in the unloaded region of the panel. This failure corresponds to a decrease of the normal stress (combined to a small friction angle on the right fault) causing a lower failure limit in the Mohr-Coulomb criteria. Looking at figures 7 and 8, we can also observe that all the fault elements at the bottom of the panel are also in shear failure. All these three codes did not show opening elements in the faults.

If we consider the figure 6, which corresponds to the case 2, in a two dimensional modelling the results will be different from one cross section place to another. Here we have supplementary information in the axial direction.

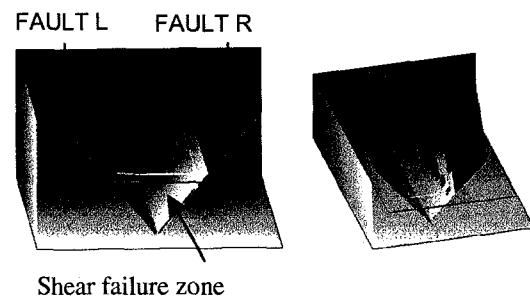


Figure 5 : Case 1 by FAULT3D

Figure 6 : Case 2 by FAULT3D

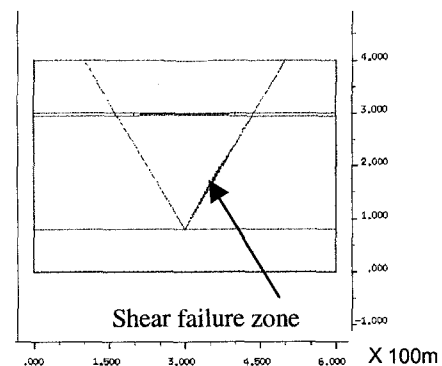


Figure 7 : Case 1 by UDEC

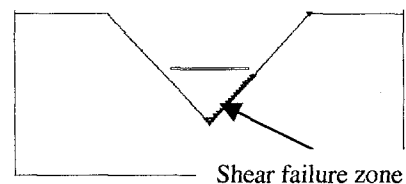


Figure 8 : Case 1 by CESAR

CESAR-LCPC : PHE2D Version 3.2.4

We can conclude, from this case, that the results given by FAULT3D are correct. Even if the calculations are in 3D, they require, here, a very low computational effort in terms of time of calculation and input data for a three-dimensional model.

#### 4 Case study : Application to a panel of Provence colliery in a faulted zone

The Provence colliery is situated in southern of France between the cities of Marseille and Aix-en-Provence. The archives found indicates that the mining began as early as the Middle Ages. Only one of the eight coal seams is presently extracted at a the depth of 1250 m. The dip of this seam is small (about  $10^\circ$ ). The roof is quite competent which assures its relative stability. This rigidity is however the source of rockbursts caused by sudden release of stored energy due to the previous stresses and the induced stresses by the excavation [1]. The other important characteristic is the presence of many faults around the mined area. For many years, numerical modelling, combined with seismic events, have been used to help predict and alleviate rockbursts or collapses due to fault slip burst [5]

##### 4.1 final panel length forecast in a faulted rock mass

This study concerns the extraction of a new panel, called T05 (figure 9). The final decision to stop the mining of this panel will depend on the behaviour of the mine structure when it comes in the vicinity of a faulted area. It was decided to make this study using FAULT3D to determine the final length of the panel which would ensure safety and profitability. The major problem is to determined the fault's characteristics from their tracks observed in the seam. Geomechanical parameters are essentially determine by the filling material properties and the fault's geometry will be estimated by orientations in the seam. This study also includes the old panels mined out before, which are T02 and T03.

##### Description of the model

The study concerns three lengths of the T05 panel (450 m, 500m and 550 m). It takes into account four faults observed during the excavation of the galleries V29 and V31 (Figure 9). Figure 2 shows the geometry of the model. The geomechanical parameters estimated for these faults are listed in the table 2.

Name	$K_n$ (MPa/m)	$K_s$ (MPa/m)	$\varphi^\circ$
A	10000	1000	$30^\circ$
B	10000	1000	$30^\circ$
C	10000	1000	$20^\circ$
D	10000	1000	$30^\circ$

These parameters are determined from in situ observations and previous analysis.

#### In Situ Stress

The in Situ Stress calculations are done using the stress tensor measured in Situ in the gallery V29 with the hydraulic fracturing method. They are :

- vertical stress : 27.5 MPa
- major horizontal stress East-West 34 MPa
- minor horizontal stress North-South 20 MPa

The elastic parameters of the rock mass in the floor and the roof are :

- Modulus of elasticity  $E = 20000$  MPa
- Poisson's ratio  $\nu = 0.25$

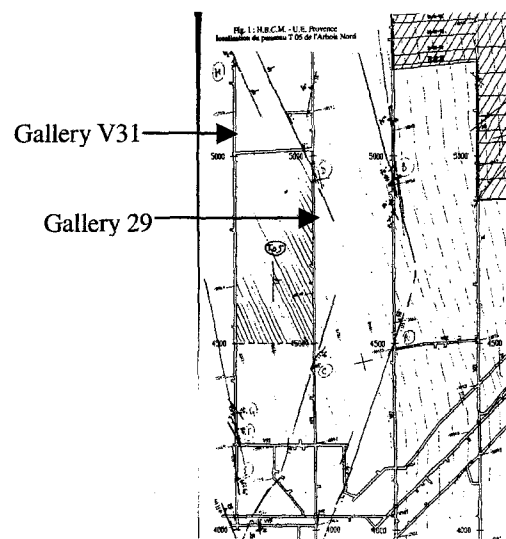


Figure 9 : map of T05 panel

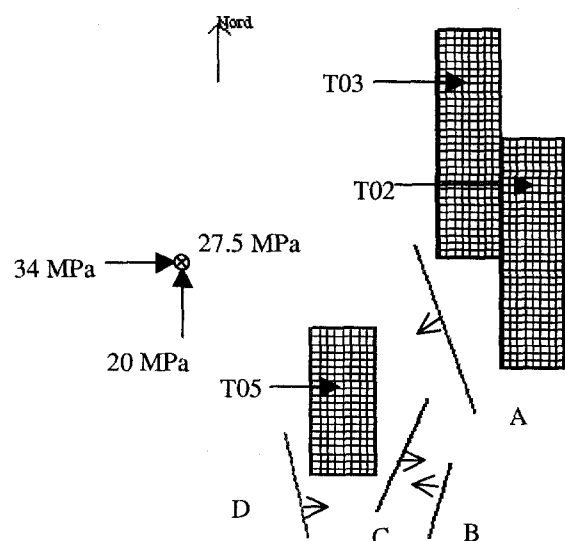


Figure 10 FAULT3D model

## Analysis of the results

### Case 1 : Mined panel of 450 m

This configuration induces a shear failure zone, only on the fault C, corresponding to 1% of the total surface of the fault plane. This zone is situated in the roof of the seam, behind the panel face and is caused by a decrease of the stress acting to the normal of this fault plane (figure 11).

### Case 2 : length of 500 m

Figure (12) shows an increase of the failure zone from 1% to 5% of the total surface of the fault C. This zone is still situated behind the face and about 100 m of the panel is concerned.

The failure zone extends above the seam until the limit of the fault. With the impossibility to know the dimensions of the fault, the only way to determine the exact failure zone is to increase the extent of the fault to incorporate the entire failure zone. That was done by increasing the extent of the fault by 50 m. This led to a new failure zone corresponding to 8 % of the total surface.

### Case 3 : length of 550 m

The progress of the panel toward the fault C induces the increase of the failure zone size to a new value corresponding to 11% of the fault surface (figure 13). In the 3 cases there is no failure in the faults A, B and D.

It appears from this study that a length of the panel less than 500 m should not affect the fault stability. For an extraction length greater than 500 m, the propagation of fault C failure affects progressively the seam when the mining face approach the fault. Thus, this situation could trigger seismic activities leading to rockburst.

### 4.2 back analysis of observed phenomena during the T05 panel excavation

Fault slip failure depends strongly on the geometry and geomechanical parameters of the fault. We mentioned that all these parameters were very difficult to estimate. During the mining of this panel, four seismic events were recorded in the side wall of V31 gallery. These events were caused either by fault D or by the failure of the rock mass. However, the stresses induced by the progress of the panel are not great enough to cause these events. In the next section we will study the influence of fault D by modifying, essentially, its dip and its azimuth.

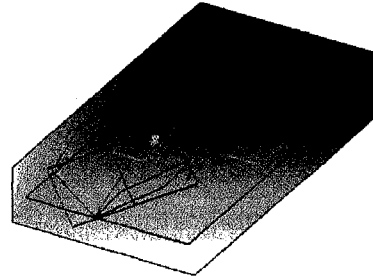


Figure 11 : panel length = 450 m

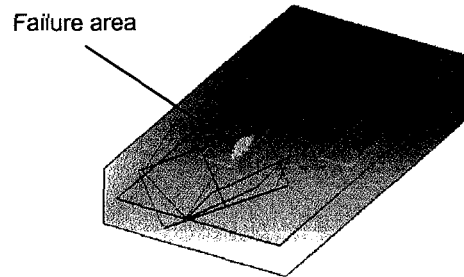


Figure 12 : panel length = 500 m

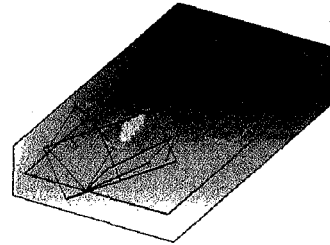


Figure 13 : panel length = 550 m

### 5 Parametric study of the fault D

As we suspect failure on the fault D to be the source of recorded events at the gallery V31, we are showing above in which case this can be possible. We consider a fixed length of 500 m and modify the dip and the azimuth of the fault in order to show the failure area. The 3 other faults are still in the same configurations.

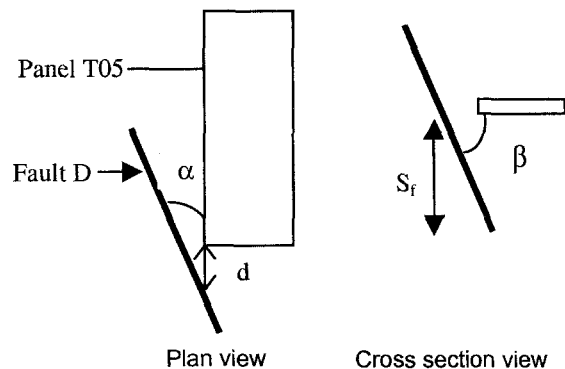


Figure 14 : parametric study of fault D

As we saw in the last calculations, only the part of the fault laying in the under stressed zone of the panel is concerned by the failure. This part of the fault, called failure surface  $S_f$ , is a function of  $\alpha$ ,  $\beta$  and  $d$  parameters. Modifying either  $\alpha$  (azimuth) or  $\beta$  (Dip) or  $d$  causes the modification of  $S_f$ . Thus, for a given friction angle ( $20^\circ$  in this study), we can find two combinations of these three parameters corresponding, respectively, to a maximum or a minimum value of  $S_f$ .

We can see that the maximum of  $S_f$  is obtained when  $\beta$  is low and becomes minimum when  $\beta$  is near  $90^\circ$ .

We represent in figures 15 and 16, the modifications observed when  $\beta$  is equal to  $75^\circ$  and when its equal to  $15^\circ$ . In the first case less than 1% of the surface is in shear failure and in the second case 8% is in shear failure and 1% in traction failure. The shear failure is caused by a decreasing of the normal stress to the fault and the traction failure by the stress concentration at the limit of the panel.

Figure 17 and 18 show a decrease of the failure zone when  $\alpha$  is modified from  $6^\circ$  to  $10^\circ$ . Values of  $\alpha$  greater than  $10^\circ$  reduce the size of  $S_f$  and consequently the number of elements prone to failure.

As a conclusion, we can say that in some cases the fault D can be at the origin of recorded events in the gallery V31. Knowing the mechanism of these events we can calibrate the fault parameters in order to retrieve the same failure mechanism on the fault and make our model more realistic for the forecasts modelling.

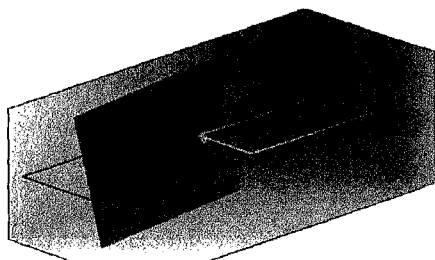


Figure 15 :  $\alpha = 6$ ,  $\beta = 75$

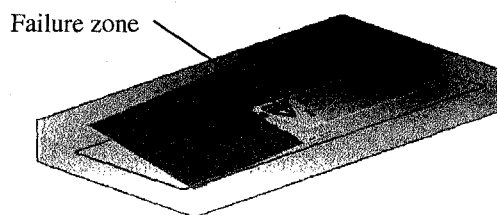


Figure 16 :  $\alpha = 6$ ,  $\beta = 15$

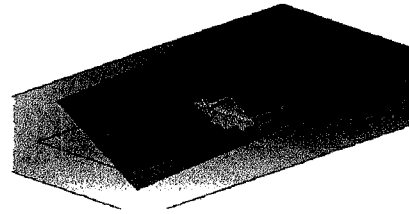


Figure 17 :  $\alpha = 6$ ,  $\beta = 35$

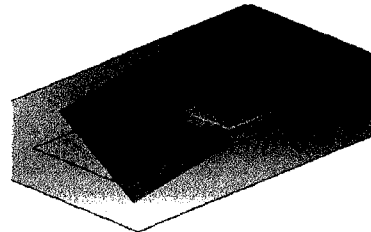


Figure 18 :  $\alpha = 10$ ,  $\beta = 35$

## 6. – Conclusion

A 3-Dimensional numerical modelling tool for underground mines excavations in faulted rock mass has been recently developed by the authors. As the only need is to discretize the panel and fault planes, the model requires little computational effort compared to other differential methods.

Developing this tool under Windows<sup>®</sup> provides us a convivial interface for input data and results view after the calculations.

The newly developed model has been verified with a single coal mining problem of a pair of faults intersecting the coal seam. The model results are in good agreement with the predictions of UDEC and CESAR commercial codes.

While the geometry of the panels is known, the major challenge is to characterise the faults and their distribution and their orientations. Also, it is important to estimate the parameters that govern their plane displacements. We show that using other methods, seismic events recorded for example, to characterise the media behaviour can permit us, by back analysis, to adjust our model (faults parameters and geometry) for future modelling.

## Acknowledgement

It was helpful for us to get exploitation information from the Provence colliery engineers. We would like to thank them for their comments and useful discussions.

This work has been financially supported by an industrial research from the Provence colliery; the authors are grateful for their support.



## 7 References

- [1] AL HEIB M., - Numerical modelling applied to dynamic phenomena – 2<sup>nd</sup> North American Rock Mechanics Symposium – June 1996 – Numerical modelling of ground burst problems – Workshop notes – Ed. Mc Gill, pp 3-1 to 3-12
- [2] CROUCH, S.L. 1979., Computer simulation of mining in faulted ground. Journal of the South African institute on mining and metallurgy. (January, pp 159-173).
- [3] FOTOOHI. K.1993, Nonlinear boundary element analysis of rock mass with discontinuities. McGill University, Montreal, Canada.
- [4] LINKOV A.M., ZOUBKOV V.V. et AL HEIB M., Computer aided in analysis of stressed state and rockburst hazard in veins and coal seams influenced by faults-Proc. Of the 1<sup>st</sup> Southern African Rock Engineering Symposium, Johannesburg, 15-17 September 1997, pp44-55. Ed SARES (ISBN NO.0-9583974-3-0).
- [5] SYLLA M., SENFAUTE G., AL HEIB M., DERRIEN Y., JOSIEN J.P.- Pr vision du comportement des terrains sous l'influence des failles par des m thodes num riques et microsismiques – The 28th Int. Conf. Of the safety in mines Research Institutes, Bucarest. 1999.